Polyethylene-Based Nanocomposite Films: Structure/Properties Relationship

Raquel E. Martini,[1] Simone La Tegola,[2] Andrea Terenzi,[2] José M. Kenny,[2] Silvia E. Barbosa[1]
[1] *IDTQ- Grupo Vinculado PLAPIQUI – CONICET, Facultad de Ciencias Exactas Físicas y Naturales, Universidad Nacional de Córdoba, Av. Vélez Sarsfield 1611, Ciudad Universitaria, 5016, Córdoba*

[2] *Materials Engineering Center, Civil and Environmental Engineering Department, University of Perugia, Località Pentima Bassa, 21, 05100 Terni, Italy*

[3] *Planta Piloto de Ingeniería Química, PLAPIQUI (UNS - CONICET) Cno. La Carrindanga Km.7 - 8000 Bahía Blanca, Argentina*

Polyethylene (PE) is the most used thermoplastic commodity as a consequence of its convenient cost-processing-performance relationship and it can be used in the form of films for food, goods and farming packaging. On the other hand, sepiolite is a high surface area and porosity hydrated magnesium silicate with both remarkable adsorptive and absorptive properties. Thus, PE and sepiolite can combine their properties synergetically to obtain new materials with enhanced properties. In this work, a systematic study of final properties of PE-sepiolite nanocomposite films was performed to investigate the influence of the sepiolite content and modification on the PE properties. Nanocomposites films with 1, 3, 5 and 10 wt % of sepiolite, with and without surface modification, were prepared by cast film extrusion and tested. The filler dispersion and distribution were evaluated by Transmission Electron Microscopy (TEM) and Fourier Transform Infrared Spectroscopy (FTIR), whereas the film crystalline morphology was analyzed using Atomic Force Microscopy (AFM), Differential Scanning Calorimetry (DSC) and X-ray Diffraction (XRD). Final properties as mechanical ones, oxygen permeability and transparency were also studied and related with the film structure. Mechanical properties, crystallization and oxygen permeability were increased maintaining good film translucency. **POLYM. ENG. SCI., 54:1931–1940, 2014.**

INTRODUCTION

The introduction of inorganic nanoparticles into polymer systems results in polymer nanocomposites exhibiting multifunctional and high-performance polymer characteristics [1]. By developing these new materials, it is possible to reach new properties and to exploit unique synergies between materials. Multifunctional features attributable to polymer nanocomposites consist of improved thermal and/or flame resistance, moisture resistance, changes in permeability, charge dissipation, and chemical resistance [1]. The improved properties are due to the interaction between polymer and clay at the nanoscale level enhanced by the huge interface area.

Polyethylene (PE) is considered one of the most used thermoplastic commodities for both industrial and consumer products. It has good mechanical properties, chemical resistance and processability. PE films constitute the largest market segment for PE and are used for food, household goods, and farming packaging. Thus, improvements in both the mechanical and changes in barrier properties of the PE films will promote and expand current applications as well as lead to more advanced applications [2].

Sepiolite is a family of fibrous hydrated magnesium silicate with the theoretical half unit-cell formula $Si_{12}O_{30}Mg_8(OH, F)_4(OH_2)_4.8H_2O$. It has a structure similar to the 2:1 layered structure of montmorillonite, formed by two tetrahedral silica sheets enclosing a central sheet of octahedral magnesia except that the layers lack continuous octahedral sheets [3]. The discontinuous nature of octahedral sheets allows for the formation of rectangular channels aligned in the direction of the a-axis, which contain some exchangeable Ca^{2+} and Mg^{2+} cations and 'zeolitic water'. The particular arrangement of atoms produces a needle-like structure, instead of typical plate-like one. The nanostructured tunnels account in large part for the high specific surface area and excellent sorption properties of sepiolite: it adsorbs vapour and odours and can absorb approximately its own weight of water and other

Correspondence to: Silvia E. Barbosa; e-mail: sbarbosa@plapiqui.edu.ar
DOI 10.1002/pen.23743
Published online in Wiley Online Library (wileyonlinelibrary.com).

liquids. In addition, it has good mechanical strength and thermal stability. These properties make sepiolite ideal for reinforcement of polymer materials such as elastomers [4, 5], thermoplastic polymers [6] and biopolymers [7].

In this sense, PE - sepiolite nanocomposites are very interesting materials because they can combine their properties synergetically to obtain new materials with enhanced properties. For example, these materials processed as films could neutralize waste odor and/or absorbed the lixiviated oil in waste bags without detriment of mechanical properties. In previous works, this kind of nanocomposites films were prepared by melt compression and the influence of different kind of nanofiller modifications on final properties was studied [8–10]. The main conclusion is that the sepiolite presence enhances both mechanical properties and film thermal stability. However, the improvement included by nanofiller modification depends on the kind of treatment. Using titanates as surface modifier, Vigo et al. [10] found not changes in film final properties. On the other hand, Saeed et al. [8] show that silanes modified sepiolites enhance the adhesion with PE and consequently, slightly improve the mechanical properties of their films.

In this work, a systematic study of nanocomposites films structure-properties relationship was performed to investigate the influence of the sepiolite content and modification on different final properties of PE. Since commercial films are usually made by blow molding or cast film extrusion, this study was carried out on nanocomposite films prepared by cast film extrusion in order to give a possible technological application in packaging industries. When compared with film prepared by melt compression, this kind of processing can introduce differences in film properties because stresses are generated during the process, inducing elongation and then polymer chain alignment. This alignment can influence crystallinity, mechanical properties and other properties dependent on these characteristics. In melt compression, the polymer flows in all direction and no preferential molecular ordering is reached. Mechanical properties, oxygen permeability and transparency of films were studied. Nanocomposites films with 1, 3, 5 and 10 wt% and using sepiolite with and without surface modification were prepared by cast film extrusion and tested. Filler dispersion and distribution were evaluated by Transmission Electron Microscopy (TEM) and Fourier Transform Infrared Spectroscopy (FTIR), whereas film crystalline morphology was analyzed using Atomic Force Microscopy (AFM), Differential Scanning Calorimetry (DSC) and X-ray Diffraction (XRD).

EXPERIMENTAL

Materials

Linear Low Density Polyethylene (PE) Dowlex 2045, kindly supplied by DOW Chemical, was used as a nanocomposite matrix. This film grade PE, adequate for heavy duty applications, has a molecular weight distribution described by Mw: 119000 g/mol, and polydispersity = 3.97. Two different grades of commercial sepiolite PRG4 and PRG5, from TOLSA-Spain, were used as nanofillers. PRG4 is a non modified mineral and PRG5 contains vinyl-trimethoxysilane as compatibilizer. Sepiolite has acicular form and their average length is around 1.5 μm and diameter of 0.01 μm. These particles contain open channels 3.6 Å x 10.6 Å in dimension running along the axis of the particle.

Compounding and Film Preparation

In order to enhance both sepiolite nanoparticles dispersion and distribution in PE matrix nanocomposite films, they were prepared in three steps by using two different twin screw extruders (TSE). Initially, masterbatches containing 10 wt% of nanofillers were compounded in a counter rotating twin screw extruder BAUSANO MD30 at 40 rpm and the following temperature profile: 135-155-170-175-185–190°C (from feed to die). The TSE was fed with a physical mixture of PE pellets and the corresponding sepiolite. Each sepiolite was previously dried under vacuum at 80°C during 24 hs. In a second step, each masterbach was diluted up to final concentration in a *DSM Micro-5&15-Compounder*, and then were pelletized. This apparatus is a co-rotating TSE with recirculation. Four concentrations of nanocomposites, containing 1, 3, 5, and 10 wt%, were prepared at 150 rpm for 1 min, with a temperature profile of 135, 160, and 190°C, from feed to die.

In the third step, films were obtained using a DSM Film Device coupled to the DSM Micro-5&15 TSE. Pellets from step two were re-extruded in the TSE using the same temperature profile. In order to obtain a constant thickness film, extrusions were performed with constant force at the head of the extruder (600 N). The cast film device comprises an air knife, a base plate, two driven rollers, a control unit and a film die of 35 mm width and 40-μm gap. The peripheral speed of the draw-off roller was 250 mm/min and a torque of 25 N-mm. The final film thickness was about 27 $\pm$ 3 μm.

Characterization

Sepiolite dispersion homogeneity was analyzed on nanocomposite pellets prepared with the final nanofiller concentration by TEM using a JEOL 100 CX equipment at 100 kV. The samples were cut in a Leica Ultracryomicrotome under liquid nitrogen. Sepiolite distribution in the films was analyzed following its relative concentration in PE using a Nicolet 520 FTIR Spectroscope. The methodology includes the comparison of typical sepiolite/PE peaks ratio in different zones of a same film. Twenty measurements were performed for each film. The peaks considered were 720 cm^{-1} for PE and 1021 cm^{-1} for sepiolite. The tolerance margin was 2%. It is important to

 DOI 10.1002/pen

note that specific controls in the films were made using a Micro-FTIR Thermo Nicolet. Then, homogeneity was assessed in the film length and width.

Crystallization analysis was performed by DSC in a Mettler Toledo 822E calorimeter. Thermograms were obtained directly on film samples heating from 25°C to 180°C and cooling from 180°C to 25°C, at a rate of 10°C/min.

Crystal orientation was analyzed by XRD in a Philips PW 1710 diffractometer, with a graphite curve monochromator, Cu anode, 45 kv, and 30 mA. Two kinds of studies were performed varying the film stretching direction respect to the X-ray beam. In one experiment, the films were placed in the sample holder parallel and in the other perpendicularly. Five spectra for sample were performed to verify the repeatability of the data obtained.

Film transparency was analyzed by UV-vis spectroscopy, in a Perkin Elmer Lambda 35 UV/VIS Spectrometer. Film Surface morphology was observed by AFM in a Nanoscope IIIa microscope (Digital Instruments) operated in Tapping Mode. In order to compare films with the same thermal history, all samples analyzed were first heated to 180°C in a Mettler microscope heating stage and then, slowly cooled under nitrogen atmosphere, with free upper surface exposed to room temperature. The lamellae thickness was assessed by using Analysis Pro Software directly on AFM images.

Tensile properties measurement was performed in a Lloyd Instruments LR 30K universal dynamometer equipped with a 50 N load-cell according to ASTM D 882-02. Ten specimens of each sample were tested at room temperature and 50 mm/min of cross velocity on strips of 10 mm of width and 100 mm of length.

Tear propagation test was performed according to ASTM D 1938-02 standard in the same dynamometer, but equipped with a 20 N load-cell. Ten specimens of 25 mm of width, 75 mm of length and notch of 50 mm were tested at room temperature and 250 mm/min.

Oxygen permeability was measured in a MOCON OX-TRAN 2/21 permeation instrument at 23°C and absence of relative humidity. Ten samples were measured for each nanocomposite and for pure PE on an exposed area of 2.5 cm^2.

RESULTS AND DISCUSSION

Nanofiller Dispersion and Distribution

TEM is a suitable technique to analyze nanofiller dispersion and distribution in a polymeric matrix. In Fig. 1, TEM images of nanocomposite pellets with 1 and 10 wt% are presented. Good dispersion and distribution is observed for nanocomposite with 1 wt% of sepiolite (Fig. 1a); however, as the nanofiller content increases, agglomerates of sepiolite appear (Fig. 1b). The latter were observed for nanocomposite with 5 and 10 wt%, while for nanocomposite with 3 wt% good dispersion is also reached. Besides, sepiolite orientation in the flow direction is evident in these images.

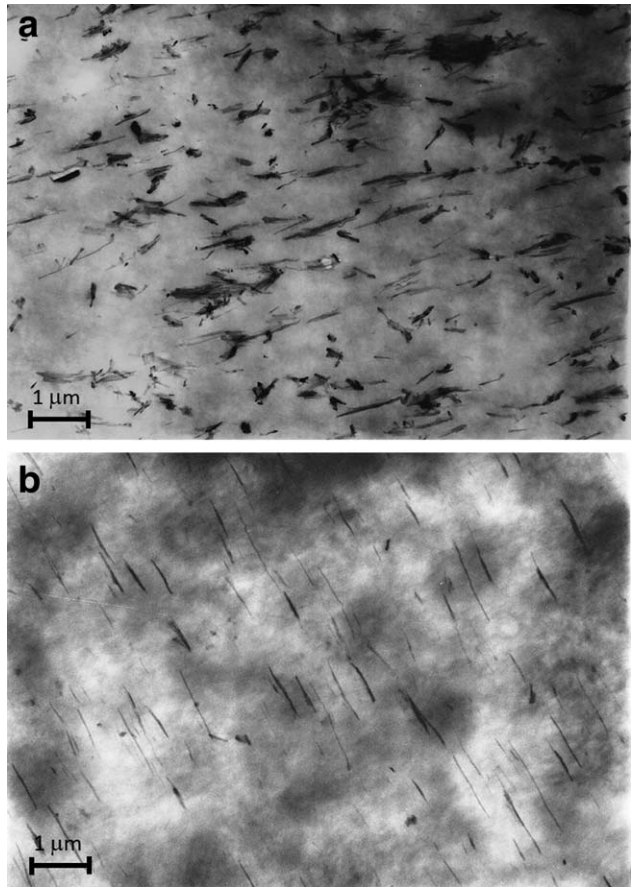

FIG. 1. TEM micrograph of nanocomposites. a) 1 wt% of PRG4 (10000 ×); b) 10 wt% of PRG4 (10000 ×).

Sepiolite dispersion in higher concentration nanocomposites can be enhanced in the third extrusion step during film preparation. Also, FTIR was applied to evaluate sepiolite distribution homogeneity in the films at "macro scale". In order to avoid the influence of the film thickness on the sepiolite distribution assessment, the sepiolite/polyethylene characteristic peaks height ratio was calculated. The sepiolite peak at 1020 cm^{-1} and the polyethylene characteristic peak at 723 cm^{-1} were selected for this calculus. This ratio was taken from different zones of the same film. In all of the measurements, a very good repeatability of this peak ratio value for a given film with particular sepiolite content was obtained indicating filler good distribution in the film. In Fig. 2, the PRG5/PE film spectra of all nanocomposites prepared are reported in comparison with the spectrum of pure PE. In the same figure, sepiolite and polyethylene peaks used for comparison are indicated. It can be observed the relative height variation of polyethylene (1470 cm^{-1} and 723 cm^{-1}) and sepiolite peaks (zones around 1000 cm^{-1} and 450 cm^{-1}) with the concentration.

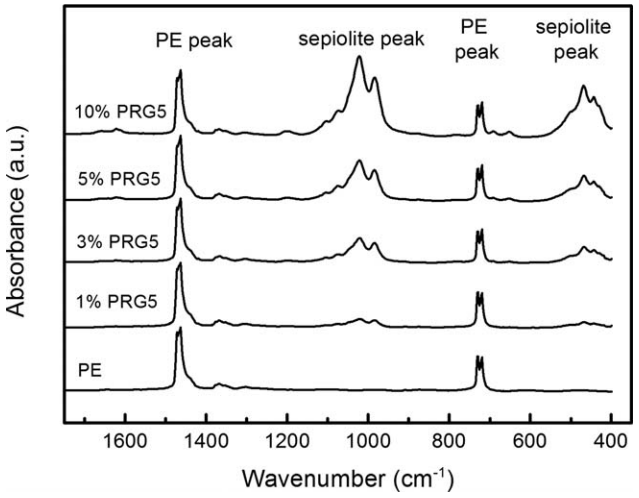

FIG. 2. FTIR spectra of nanocomposites prepared with PRG5 compared with pure PE.

Morphological Study

Final properties of nanocomposites are strongly dependent on the crystallization degree and final crystalline morphology. In Table 1, values of the crystallization degree of each film prepared obtained by DSC analysis are reported. Evidently, sepiolite acts as nucleating agent increasing the crystallization degree with respect of pure PE. However, this variation seems to be independent of the sepiolite amount. The crystallization degree increases from 35% to 44% when 1 wt% of sepiolite is introduced in PE, but then it remains constant for 3, 5, and 10% of sepiolite. This behavior was found by several authors with other nucleation agents [11, 12]. They claim that there is a saturation effect in the nucleation process with the addition of around 1 wt% of nanofillers.

To analyze possible variations in the crystalline morphology with the introduction of the acicular nanofiller, an AFM study was performed on PE and all the nanocomposites prepared. Results from topographic and phase AFM images are shown in Figs. 3 and 4. Pure PE seems to crystallize in the form of spherulites. This is expected as typical PE crystallization includes a sequential buildup of crystals. Initially a dominant spherulite growing is observed, followed by in-filled secondary lamellae formation mainly at spherulite boundaries [13]. Lamellae formation seems to be the preferential crystallization mode as the sepiolite amount increase. For nanocomposite with 1 wt% the presence of lamellar crystals is more evident and the typical spherulite crystallization seems to decrease. Intermediate structures were observed for nanocomposites with 3 and 5 wt% of sepiolite, while practically a complete oriented lamellar morphology was obtained for materials with 10 wt% of nanofiller. It is worth noticing that as sepiolite content increases, lamellar thickness decreases from around 40 nm for films with 1% of sepiolites to 20 nm for films with around 10% of nanofillers. Also, in the images (Fig. 4), a gradual preferential orientation can be observed as sepiolite content increases.

The above observations can be interpreted in terms of the nanofiller effects on crystal type induction. Acicular particles induce transcrystallinity around them. In this sense, lamellae grow from the nanofillers surface and along its axis. Transcrystallinity and spherulitic crystallization process are competitive, then as sepiolite content increases, the amount of spherulitic crystals decreases. The above claim allows us to understand the changes in crystal types and the observed lamellae orientation following the nanofiller orientation induced by the flux. However, it does not explain the decrease in lamellae thickness. One possible explanation to this behavior is that nanocomposites also present a sequential crystal buildup with an initial transcrystalline lamellar growth from higher nucleating surface the sepiolite; and in a second step, the "covered" sepiolite acts as nucleating for thinner secondary lamella [13].

These observations are in agreement with the results obtained by DSC analysis. In Fig. 5, the thermograms of nanocomposites prepared with non modified sepiolite are compared with pure PE. Two populations of lamellae are noticeable, one containing more perfect crystals with higher melting temperature, and the other one presenting thinner and defective lamellae with lower melting temperature. The sepiolite produces thinner crystal population increase, as it was also observed by AFM, while the peak corresponding to the more perfect crystal is reduced.

To complete the morphological study and corroborate the above results, XRD analysis was performed placing the films with stretching direction parallel and perpendicular to the beam to detect differences in crystal morphology with the flow direction. Figure 6 shows the XRD spectra obtained for pure PE films, sepiolite and nanocomposites. PE usually crystallizes in orthorrombic and monoclinic crystal structure [14, 15]. The XRD pattern of pure PE film obtained perpendicular to the beam is characterized by three strong peaks of (110) and (020) planes corresponding to orthorhombic phase (Fig. 6a). These peaks are individually located at 2θ values of 21.3° and 36.5°, respectively. Sepiolite is a crystalline silicate with crystal main reflection peak at 7.1°. In nanocomposites, the height of this peak is proportional to the sepiolite concentration as observed in Fig. 6a. Furthermore, in nanocomposite films analyzed with the film stretching direction perpendicular to the beam, two peaks, typical of monoclinic phase, appear at 13.8° and 16.7°. The intensity of these peaks increases as the sepiolite content is

TABLE 1. Crystallization degree of nanocomposite films.

	Crystallinity degree (%)	
Sample	PRG4	PRG5
PE	35	35
3%	44	43
5%	44	44
10%	41	43

DOI 10.1002/pen

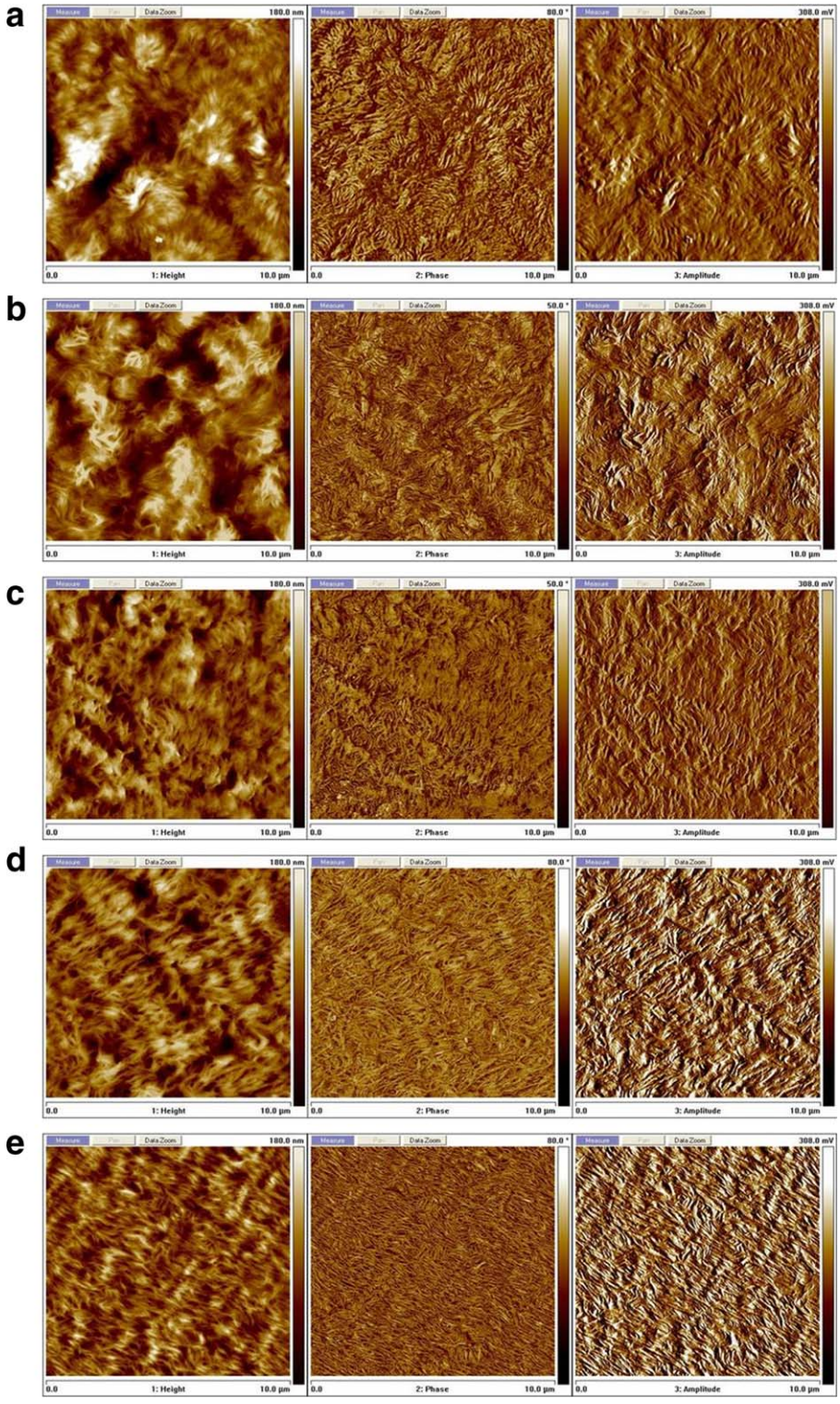

FIG. 3. AFM images of nanocomposites. a) pure PE, b) 1 wt% of PRG5, c) 3 wt% of PRG5, d) 5 wt% of PRG5 and e) 10 wt% of PRG5. [Color figure can be viewed in the online issue, which is available at wileyonlinelibrary.com.]

increased, evidencing that sepiolite favors PE crystallization in monoclinic phase when it is in perpendicular direction to the film flow direction.

Figure 6b shows the patterns obtained with the beam in parallel direction to the film stretching direction. PE patterns also present the two peaks (13.8° and 16.7°)

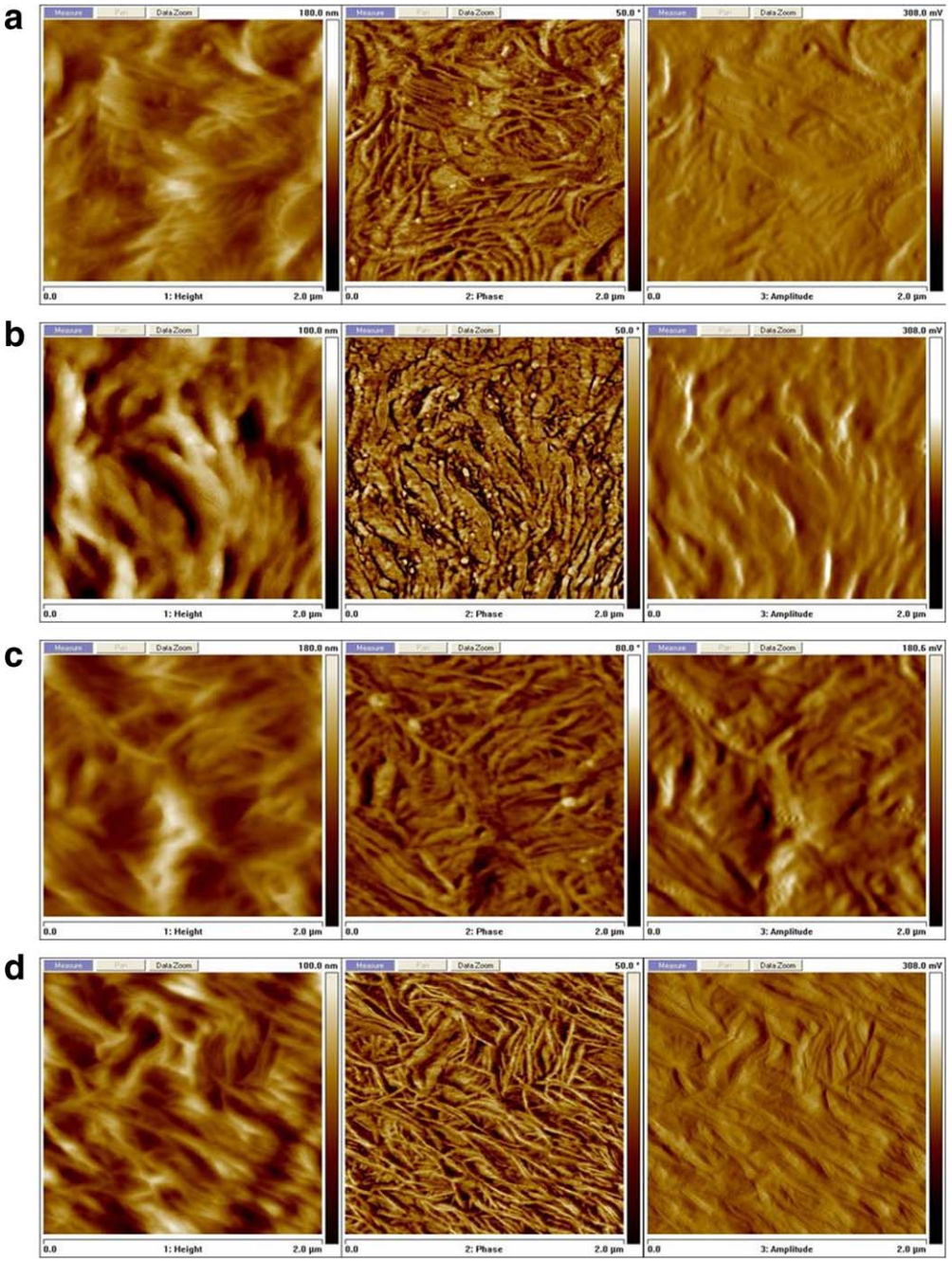

FIG. 4. Magnified AFM images of nanocomposites. a) 1 wt% of PRG5, b) 3 wt% of PRG5, c) 5 wt% of PRG5 and d) 10 wt% of PRG5. [Color figure can be viewed in the online issue, which is available at wileyonlinelibrary.com.]

corresponding to the monoclinic phase, indicating a crystal induction in flow direction due to stretching during processing. This monoclinic crystal induction in nanocomposites films seems not to be important as no differences are observed in their spectra respect to pure PE one. However, a difference is observed in the height of the peaks corresponding to the plane 110 of the orthorrombic phase, showing an increase as the nanofiller amount is increased, thus evidencing the polymer crystal orientation. The sepiolite presence in nanocomposite films is also detected for the peak at 7.1°, and additionally by the presence of other sepiolite characteristic peaks at 23.7° and 26.7°. Comparing these patterns with those obtained in perpendicular ways, a sepiolite orientation can be also detected by a higher relative intensity of sepiolite peaks respect the PE characteristic peaks (21.3°), confirming the detected sepiolite orientation in the flow direction. This changes observed in

 DOI 10.1002/pen

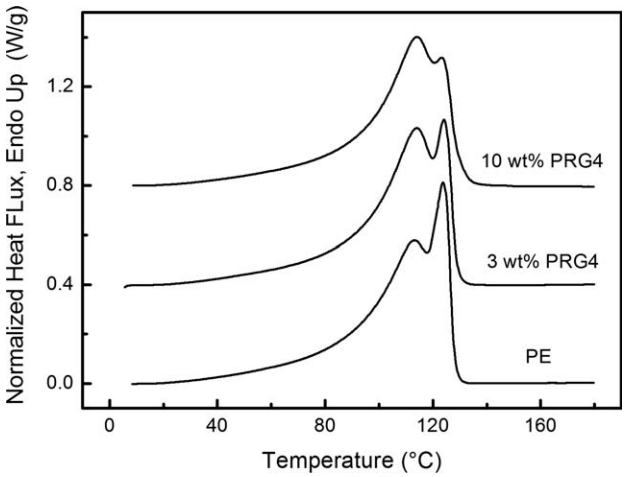

FIG. 5. DSC thermograms of nanocomposites prepared with PRG4 (3 wt% and 5 wt%) compared with pure PE.

X-ray analysis agrees with the preferential orientation observed in AFM images.

Mechanical Properties

In Table 2, the Young's Modulus (E) of all nanocomposite films prepared, including pristine PE are reported. As expected, there is an increment of the E with the sepiolite content, achieving an increase of 77% for the nanocomposites with 10 wt% PRG5. This result is attributed to both the nanofillers presence (rigidity) and their effect on PE crystallization, as mentioned above. The most important increment is observed when the sepiolite content varies from 1 to 3 wt%, and from then, the increment is less pronounced. Taking into account that the nanocomposites crystallization degree does not change significantly at high sepiolite concentration, it is reasonable to think that the effect of sepiolite on the crystallization dominates mechanical properties behavior.

The rigidity of the nanocomposites prepared with modified sepiolite is slightly higher -except for samples with 5 wt% of sepiolite-, probably due to the better adhesion filler-matrix. However, observed differences are within the limits of experimental error.

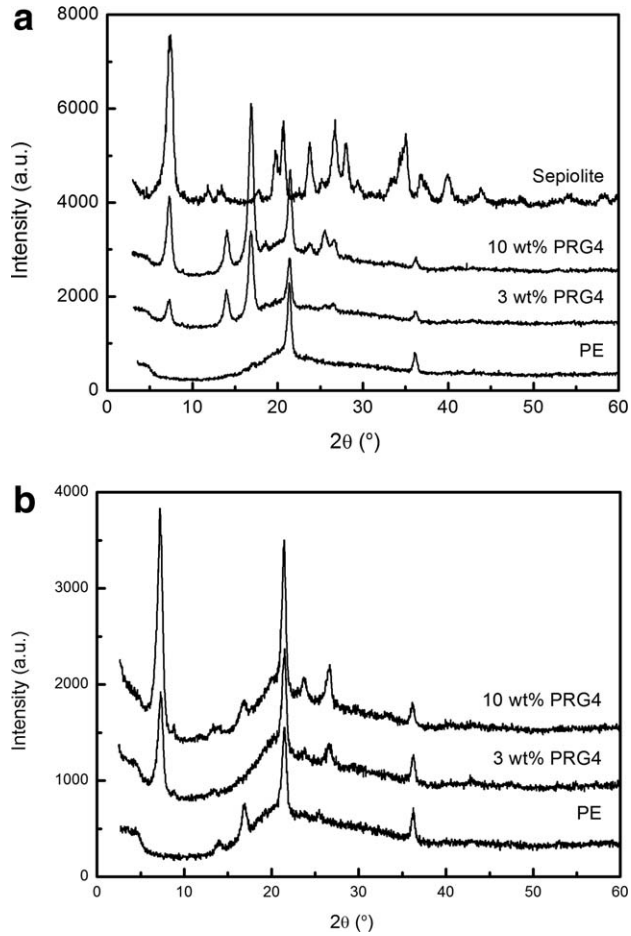

FIG. 6. X-ray diffraction patterns of nanocomposite film prepared with different sepiolite amount compared with pure PE. a) Film direction perpendicular to the beam, b) Film direction parallel to the beam.

Moreover, the filler presence produces a faint increase in the yield strength (shown in Table 2) although the yield strain is nearly the same for pure PE and nanocomposites. On the other hand, no clear tendency is observed in tensile strength variation with sepiolite content (Table 2). However, if a comparison of stress–strain curves is performed (Fig. 7), nanocomposite stress–strain curves lie over the neat PE one, bearing higher stresses as the sepiolite

TABLE 2. Mechanical properties of nanocomposite films.

Material	Young Modulus (MPa)	St. Dev.	Yield Strength (MPa)	St. Dev.	Tensile Strength (MPa)	St. Dev.	Elongation at break (%)	St. Dev.
PE	173.42	7.78	7.22	0.33	38.16	7.06	434.13	49.20
1 wt% PRG4	185.40	17.36	6.80	0.83	26.19	4.52	301.91	31.81
3 wt% PRG4	259.58	19.28	8.22	0.46	38.94	7.84	333.19	40.74
5 wt% PRG4	279.98	28.02	8.68	0.42	36.15	6.44	329.81	35.18
10 wt% PRG4	255.92	21.08	7.84	0.44	31.08	5.18	376.68	51.04
1 wt% PRG5	204.06	16.49	7.64	0.54	29.59	7.71	328.38	56.68
3 wt% PRG5	268.28	31.99	8.60	0.55	40.35	8.48	350.99	54.54
5 wt% PRG5	258.18	19.31	8.44	0.29	42.36	8.31	398.46	39.13
10 wt% PRG5	308.00	15.92	9.36	0.25	35.08	3.60	381.36	16.60

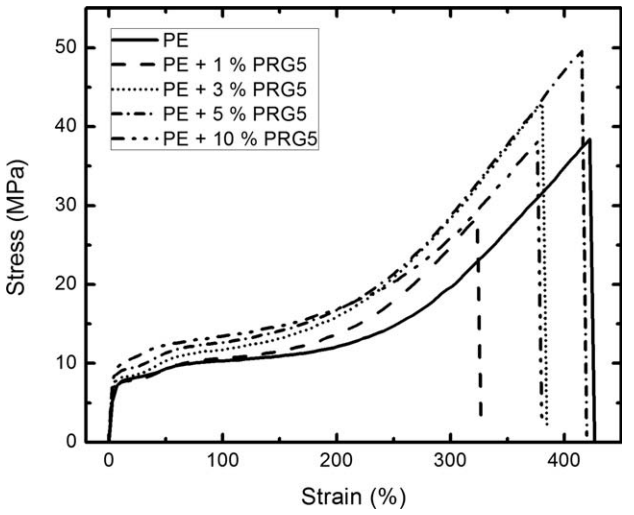

FIG. 7. Stress-strain curves for nanocomposites films prepared with PRG5 compared with pristine PE.

content increases. Curves have the typical behavior observed in oriented ductile material measured in parallel direction of the orientation [16]. Also, it is noticed that the nanocomposites film break at lower strain than pristine PE. Average values of strain to failure for each sample are reported in Table 2. Hence, in this case, the maximum stress and then the tensile strength corresponds to the fracture point. Therefore, the unclear trend of tensile strength might be due to the lower strain to failure of nanocomposites films and the possibly related PE-interphase failure. It is important to note that the strain to failure decreases for nanocomposites, but this decrement is small, 30% as maximum respect to pure PE, and all films remain flexible with an elongation at break higher than 300%. In addition, it is very interesting to perform a detailed analysis of Fig. 7. For strains higher than 200%, the stress–strain curve for nanocomposites with 10 wt% of sepiolite crosses the 3 and 5 wt% curves, withstanding lower stresses. This fact can be due to the presence of more imperfect crystals with thinner lamellae in nanocomposites as sepiolite content increases, hindering lower stresses. Besides, it can be observed that the curves of pure PE and nanocomposites with 1 wt% of sepiolite match up to a strain of *circa* 75% and after that, the nanofiller reinforcement is evident. The "amount" of amorphous phase is similar in PE and nanocomposites with 1 wt% of sepiolite, then as this phase is the first to extend at low strain, the matching of this curves in this zone can be explained. As the strain increases, the crystalline phase begins to stretch and its effect in nanocomposites is evident.

A critical requirement for polymeric film in applications like packaging is the tear resistance. In Fig. 8, tear resistance of nanocomposites is compared with the resistance of pure PE. In general, this value decreases *ca*. 30% for all composites when PRG4 sepiolite is used. However, for nanocomposites prepared with compatibilized sepiolite, higher values of tear resistance are obtained with nanocomposites films with 1 and 10 wt% nanofiller content. However, the main difference detected in this test was tear propagation behavior. In films prepared with pristine PE, tear propagates transversally to the cut direction; instead, in nanocomposites films, tear propagates in the same direction of the cut. For nanocomposites prepared with 1 wt% of sepiolite an intermediate behavior was observed: some specimens break in transversal direction and others in the same direction. The tear propagation test was performed in the same direction of film stretching, this difference in the crack propagation can be understood considering the sepiolite and polymer crystal orientation in the film stretching direction as demonstrated above. Thus, in nanocomposite films, the cut propagates parallel to the larger dimension of the filler. This propagation is also favored by the crystallization in lamellar structure form with preferential orientation, as previously discussed. On the other hand, the transversal propagation can be expected in materials that crystallize mainly with spherulitic structure, such as PE films since cracks proceed between the spherulite edges. The sepiolite orientation and the lamellar structure can also explain tear strength reduction because the test is performed in the film machine drawing direction.

Oxygen Permeability

Oxygen permeability through the film is an important factor in packaging applications, as it determines the shelf-life of many packed foods. The value of oxygen permeability for each kind of film prepared is reported in Table 3. Permeability increases as the sepiolite increases, except for nanocomposites prepared with modified sepiolite where the maximum value is reached for nanocomposites with 5 wt% of filler. The increment in oxygen permeability proceeds from the nature of sepiolites. They have a porous structure with channels and OH in the surface, as shown in Fig. 9 [17]. This structure favors the

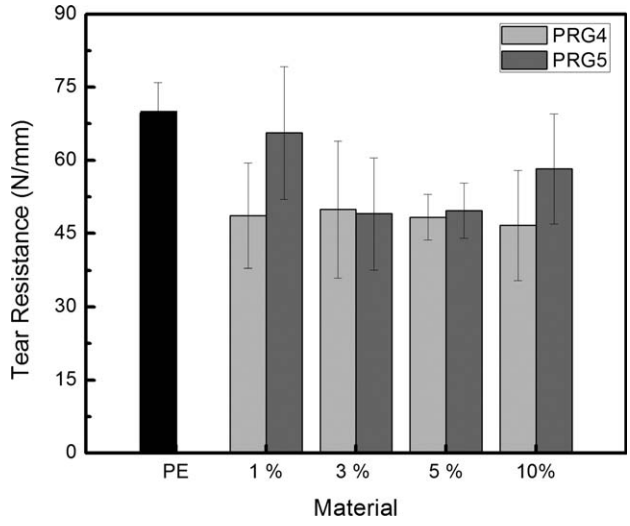

FIG. 8. Tear resistance of nanocomposites films prepared with PRG4 and PRG5 sepiolite compared with pristine PE.

 DOI 10.1002/pen

TABLE 3. Oxygen permeability of pure PE and nanocomposite.

Sample	OP (cc mil/m^2 day)	St. Dev.
PE	8,231	171
1wt% PRG4	7,706	372
3 wt% PRG4	11,208	460
5 wt% PRG4	11,036	531
10 wt% PRG4	11,478	544
1 wt% PRG5	9,741	457
3 wt% PRG5	10,465	493
5 wt% PRG5	13,052	612
10 wt% PRG5	11,094	524

oxygen pass by physicochemical interactions. Also, the oxygen path impediment by the tortuosity, typical in clay nanocomposites, is less in these nanocomposites. Sepiolite has one dimension higher than the other two due to the needle-like shape, then the tortuosity is not highly incremented by the inclusion of this kind of filler. In common clay nanocomposites, platelet-shaped filler are used as fillers; then, the impermeable clay layers force a tortuous pathway for a permeant through the nanocomposites film, incrementing barrier properties [18].

This particular behavior found in sepiolite/polyethylene films is very useful in applications where there is a need to interchange gases from and to the package, i.e. in packaging of breathing products as fruits and vegetables. Water and carbon dioxide permeability must also be analyzed to evaluate its applications in modified atmosphere/modified humidity packaging. Controlling the sepiolite amount and the surface sepiolite modification, a film can be designed for specific applications.

Transparency

Transparency of film is one of the aesthetic factors enhancing general appearance and customer acceptance. Generally, transparency of the film would decrease when adding micro particles; in fact, nanocomposite film transparency depends on the clay dispersion and amount of clay.

UV transmission percentage of nanocomposites prepared with non modified sepiolite is reported in Fig. 10.

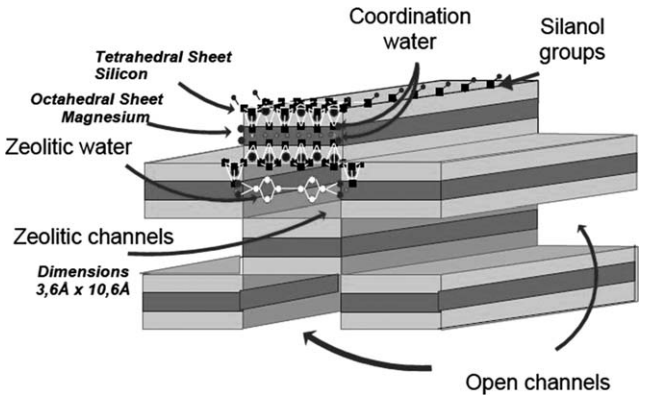

FIG. 9. Sepiolite structure [17]

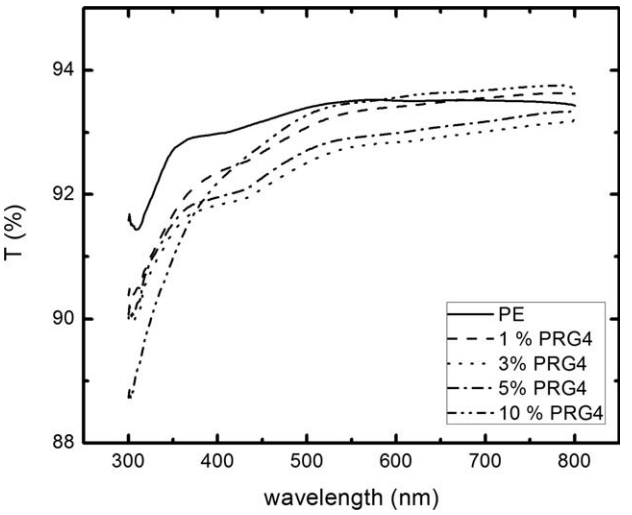

FIG. 10. UV-vis spectra of nanocomposite films prepared with PRG4.

It is observed that the transmittance, and hence film transparency is reduced with the filler presence. However, these differences are remarked due to the graph scale and the differences in transmittance for a wavelength value do not exceed 1%, and for all nanocomposites the transmittance are between 91 and 94% for all range analyzed, concluding that the small loadings practically do not affect the film clarity. Not important differences were detected for materials prepared with modified sepiolite. This result is also an additional evidence of good filler dispersion.

CONCLUSIONS

In this work, nanocomposite films of linear low density polyethylene with different amount of sepiolite nanofillers up to 10% were prepared. Both sepiolite with and without surface modification were used. It was demonstrated that good dispersion and distribution was obtained for both kinds of material.

Sepiolite increased the crystallization degree and induced changes in crystal morphology and orientation. Its presence increased the thinner crystal population and favored crystallization in monoclinic phase perpendicular to the film flow direction. On the other hand, a preferential alignment of PE ortorrombic phase crystal was observed in longitudinal film direction due to the film stretching.

The mechanical properties of the nanocomposites were improved with respect to pure PE and increased with the filler amount. However, the elongation at break decreased although the nanocomposites films remained flexible for all the compositions studied, with an elongation at break higher than 300%. The effect of the nanofiller was not detected in tear propagation tests, probably as a consequence of the orientation of the nanofiller in the direction of the test, parallel to film stretching. However, a difference in tear propagation behavior was observed. In films prepared with pristine PE the tear propagated transversally

to cut direction instead, in nanocomposites films, tear propagated in the same direction of notch. Oxygen permeability increased as the nanofiller amount increases due to the porous structure of sepiolite with OH in surface.

The small loading practically did not affect film transparency. With the filler addition films lost shine and some clouding was produced for higher sepiolite contents where agglomerates presence could be possible.

The sepiolite compatibilization did not introduce important changes in nanocomposites properties. Only a slight increment in reinforcement efficiency is observed for compatibilized sepiolite, showing that the properties of the polyethylene are improved by the mere presence of the sepiolite. The last matter is another benefit of the present system because a good dispersion and distribution of clay in sepiolite is obtained without compatibilization, allowing to obtain films with enhanced properties and low costs.

REFERENCES

1. J. Koo, *Polymer Nanocomposite. Processing, Characterization and Applications*, Mc Graw-Hill, New York (2006).
2. S.M. Ali Dadfar, I. Alemzadeh, S.M. Reza Dadfar, and M. Vosoughi, *Mater. Des.*, **32**, 1806 (2011).
3. S. Xie, S. Zhang, F. Wang, M. Yang, R. Séguéla, and J.M. Lefebvre, *Compos. Sci. Technol.*, **67**, 2334 (2007).
4. L. Bokobza, A. Burr, G. Garnaud, M. Perrin, and S. Pagnotta, *Polym. Int.*, **53**, 1060 (2004).
5. L. Bokobza, *J. Appl. Polym. Sci.*, **93**, 2095 (2004).
6. S. La Tegola, A. Terenzi, R. Martini, S. Barbosa, L. Torre, and J. Kenny, *Macromol. Sympo.*, **301**, 128 (2011).
7. M. Darder, M. Lopez-Blanco, P. Aranda, A.J. Aznar, J. Bravo, and E. Ruiz-Hitzky, *Chem. Mater.*, **18**, 9 (2006).
8. M. Shafiq, T. Yasin, and S. Saeed, *J. Appl. Polym. Sci.*, **123**, 1718 (2012).
9. N. García, M. Hoyos, J. Guzmán, and P. Tiemblo, *Polym. Degrad. Stabil.*, **94**, 39 (2009).
10. M. Arroyo, F. Perez, and J.P. Vigo, *J. Appl. Polym. Sci.*, **32**, 5105 (1986).
11. L.A. Castillo, S.E. Barbosa, and N.J. Capiati, *J. Appl. Polym. Sci.*, **126**, (2012).
12. C. Albano, J. Papa, M. Ichazo, J. González, and C. Ustariz, *Compos. Struct.*, **62**, 291 (2003).
13. C. Frederix, J.M. Lefebvre, C. Rochas, R. Séguéla, and G. Stoclet, *Polymer*, **51**, 2903 (2010).
14. D. Olmos, C. Domínguez, P.D. Castrillo, and J. Gonzalez-Benito, *Polymer*, **50**, 1732 (2009).
15. Q. Yuan, R. Gudavalli, and R.D.K. Misra, *Mater. Sci. Eng. A*, **492**, 434 (2008).
16. L.E. Nielsen and R.F. Landel, *Mechanical Properties of Polymers and Composites*, M. Dekker, (1994).
17. S. La Tegola, *Influence of processing conditions in mechanical and rheological properties of PP/high aspect-ratio particles nanocomposites and their effects on drawability of nanocomposites fibers*, Ph D Thesis, Università degli Studi di Perugia. Facoltà di Ingegneria Polo di Terni (2008).
18. G. Choudalakis and A.D. Gotsis, *Eur. Polym. J.*, **45**, 967 (2009).

 DOI 10.1002/pen